PERGAMON

International Journal of Heat and Mass Transfer 45 (2002) 4281–4288

International Journal of HEAT and MASS TRANSFER

www.elsevier.com/locate/ijhmt

# Radiation and mass transfer effects on flow of an incompressible viscous fluid past a moving vertical cylinder

P. Ganesan *, P. Loganathan

*School of Mathematics, Anna University, Chennai 600 025, India*

Received 11 November 2001; received in revised form 3 April 2002

**Abstract**

The interaction of free convection with thermal radiation of a viscous incompressible unsteady flow past a moving vertical cylinder with heat and mass transfer is analyzed. The fluid is a gray, absorbing–emitting but non-scattering medium and the Rosseland approximation is used to describe the radiative heat flux in the energy equation. The governing equations are solved using an implicit finite-difference scheme of Crank–Nicolson type. Numerical results for the transient velocity, the temperature, the concentration, the local as well as average skin-friction, the rate of heat and mass transfer are shown graphically. It is found that at small values of the Prandtl number and radiation parameter $N$, the velocity and temperature of the fluid increases sharply near the cylinder as the time $t$ increase, which is totally absent in the absence of radiation effects. 

*Keywords:* Finite-difference scheme; Moving vertical cylinder; Radiation

## 1. Introduction

Many investigators have studied two-dimensional laminar boundary layer flow and convective heat transfer. Not much attention has been given, however, to cases where thermal radiation becomes an additional factor. Recent developments in hypersonic flight, missile reentry, rocket combustion chambers, power plants for interplanetary flight and gas cooled nuclear reactors, have focused attention on thermal radiation as a mode of energy transfer, and emphasized the need for an improved understanding of radiative transfer in these processes.

Studies with interaction of thermal radiation and free convection were made by Arpaci [1], Cess [4], Cheng and Ozisik [5], Bankston [2], Raptis [16], Hossian and Takhar [10,11]. In all these papers, the flow is considered steady. The unsteady flow past a moving plate in the presence of free convection and radiation were studied by Monsour [13], Raptis and Perdikis [15], Das et al. [7], Grief et al. [9] and Cogley et al. [6]. The combined radiation and free convection flow over a vertical cylinder was studied by Yih [18]. In the literature very few authors studied the flow past a vertical or horizontal circular cylinder. Studies of free convection flow along a vertical or horizontal cylinder are important in the field of geothermal power generation and drilling operations where the free-stream and buoyancy-induced fluid velocities are of roughly the same order of magnitude.

In the context of space technology and in processes involving high temperatures, the effects of radiation are of vital importance. Novotny and Kelleher [14] presented a laminar free convection of an absorbing–emitting gas in the region of stagnation point of a horizontal cylinder. Hossain et al. [12] reported the radiation–conduction interaction on mixed convection from a horizontal circular cylinder. They were using local non-similarity variables to solve the problem. The governing equations were solved numerically using implicit finite-difference scheme of Keller Box method. Recently, combined heat and mass transfer effects on moving vertical cylinder that of steady and unsteady flow were

* Corresponding author. Tel.: +91-44-2351126x3143; fax: +91-44-2350397.

*E-mail addresses:* ganesan@annauniv.edu (P. Ganesan), ploknath@hotmail.com (P. Loganathan).

0017-9310/02/$ - see front matter 
PII: S0017-9310(02)00140-0

**Nomenclature**

| | |
|---|---|
| $C$ | species concentration |
| $D$ | binary diffusion co-efficient |
| $Gr$ | thermal Grashof number |
| $Gc$ | modified Grashof number |
| $g$ | acceleration due to gravity |
| $N$ | radiation parameter |
| $\overline{Nu}$ | average Nusselt number |
| $Nu_X$ | local Nusselt number |
| $Pr$ | Prandtl number |
| $q_r$ | radiative heat flux |
| $R$ | dimensionless radial co-ordinate |
| $r_0$ | radius of cylinder |
| $Sc$ | Schmidt number |
| $\overline{Sh}$ | average Sherwood number |
| $Sh_X$ | local Sherwood number |
| $T$ | temperature |
| $t$ | time |
| $U$, $V$ | dimensionless velocity components in $X$, $R$ directions respectively |
| $X$ | dimensionless axial co-ordinate |

*Greek symbols*

| | |
|---|---|
| $\alpha$ | thermal diffusivity |
| $\beta$ | volumetric coefficient of thermal expansion |
| $\beta^*$ | volumetric coefficient of expansion with concentration |
| $\kappa^*$ | mean absorption coefficient |
| $\upsilon$ | kinematic viscosity |
| $\rho$ | density |
| $\sigma$ | Stefan–Boltzmann constant |
| $\tau_X$ | local skin-friction |
| $\overline{\tau}$ | average skin-friction |

*Subscripts*

| | |
|---|---|
| w | condition on the wall |
| $\infty$ | free-stream condition |

analyzed by Takhar et al. [17] and Ganesan and Loganathan [8]. They were using an implicit finite-difference scheme of Crank–Nicolson type.

The problem of radiation effects on free convection flow past a moving vertical cylinder has important applications in the study of geological formations; in the exploration and thermal recovery of oil; and in the assessment of aquifers, geothermal reservoirs and underground nuclear waste storage sites. Here intrusive magma may be taken as an isothermal vertical cylinder with impulsive motion subject to radiative flux. Hence, it is proposed to study the radiation effects of heat and mass transfer on the natural convection of an incompressible viscous fluid past a moving semi-infinite isothermal vertical cylinder in the vertically upward direction.

## 2. Mathematical analysis

Considered the flow of an incompressible viscous radiating fluid past an impulsively started semi-infinite vertical cylinder of radius $r_0$. Here the $x$-axis is taken along the axis of cylinder in the vertical direction and the radial coordinate $r$ is taken normal to the cylinder. It is also assumed that the radiation heat flux in the $x$-direction is negligible as compared to that in the radial direction. The viscous dissipation is also assumed to be negligible in the energy equation due to slow motion of the cylinder. All physical properties are assumed to be constant except for the density in the buoyancy term, which is given by the usual Boussinesq approximation. Under these assumptions, the flow of a radiative fluid can be shown to be governed by the following system of equations:

$$\frac{\partial(ru)}{\partial x}+\frac{\partial(rv)}{\partial r}=0 \tag{1}$$

$$\frac{\partial u}{\partial t'}+u\frac{\partial u}{\partial x}+v\frac{\partial u}{\partial r}=g\beta(T'-T'_\infty)+g\beta^*(C'-C'_\infty)+\frac{\upsilon}{\alpha}\frac{1}{r}\frac{\partial}{\partial r}\left(r\frac{\partial u}{\partial r}\right) \tag{2}$$

$$\frac{\partial T'}{\partial t'}+u\frac{\partial T'}{\partial x}+v\frac{\partial T'}{\partial r}=\frac{k}{\rho C_p}\frac{1}{r}\frac{\partial}{\partial r}\left(r\frac{\partial T'}{\partial r}\right)-\frac{1}{\rho C_p}\frac{1}{r}\times\frac{\partial}{\partial r}(rq_r) \tag{3}$$

$$\frac{\partial C'}{\partial t'}+u\frac{\partial C'}{\partial x}+v\frac{\partial C'}{\partial r}=\frac{D}{r}\frac{\partial}{\partial r}\left(r\frac{\partial C'}{\partial r}\right) \tag{4}$$

Initial and boundary conditions are

$$\begin{aligned}
&t'\leqslant 0: u=0,\ v=0,\ T'=T'_\infty,\ C'=C'_\infty \\
&\quad \text{for all } x\geqslant 0 \text{ and } r\geqslant 0 \\
&t'\geqslant 0: u=u_0,\ v=0,\ T'=T'_w,\ C'=C'_w \\
&\quad \text{at } r=r_0, \\
&u=0,\ v=0,\ T'=T'_\infty,\ C'=C'_\infty \\
&\quad \text{at } X=0 \text{ and } r\geqslant r_0 \\
&u\to 0,\ T'\to T'_\infty,\ C'\to C'_\infty \quad \text{as } r\to\infty.
\end{aligned} \tag{5}$$

We now assume Rosseland approximation (Brewster [3]), which leads to the radiative heat flux $q_r$ is given by

$$q_r = -\frac{4\sigma}{3\kappa^*}\frac{\partial T'^4}{\partial r} \tag{6}$$

where $\sigma$ is the Stefan–Boltzmann constant and $\kappa^*$ is the mean absorption coefficient.

If temperature differences within the flow are sufficiently small such that $T'^4$ may be expressed as a linear function of the temperature, then the Taylor series for $T'^4$ about $T'_\infty$, after neglecting higher order terms, is given by

$$T'^4 \cong 4T'^3_\infty T' - 3T'^4_\infty \tag{7}$$

In view of Eqs. (6) and (7), Eq. (3) reduces to

$$\frac{\partial T'}{\partial t'} + u\frac{\partial T'}{\partial x} + v\frac{\partial T'}{\partial r} = \frac{k}{\rho C_p}\frac{1}{r}\frac{\partial}{\partial r}\left(r\frac{\partial T'}{\partial r}\right) + \frac{16\sigma T'^3_\infty}{3\rho C_p\kappa^*} \times \frac{1}{r}\frac{\partial}{\partial r}\left(r\frac{\partial T'}{\partial r}\right) \tag{8}$$

The following dimensionless parameters are defined:

$$U = \frac{u}{u_0}, \quad R = \frac{r}{r_0}, \quad X = \frac{x\upsilon}{u_0 r_0^2}, \quad V = \frac{vr_0}{\upsilon},$$
$$t = \frac{t'\upsilon}{r_0^2}, \quad T = \frac{T' - T'_\infty}{T'_w - T'_\infty}, \quad C = \frac{C' - C'_\infty}{C'_w - C'_\infty},$$
$$Gr = \frac{g\beta r_0^2(T'_w - T'_\infty)}{\upsilon u_0}, \quad Gc = \frac{g\beta^* r_0^2(C'_w - C'_\infty)}{\upsilon u_0},$$
$$Pr = \frac{\mu C_p}{k}, \quad N = \frac{\kappa^* k}{4\sigma T'^3_\infty}, \quad Sc = \frac{\upsilon}{D} \tag{9}$$

With the non-dimensional variables (9), Eqs. (1), (2), (8) and (4) become

$$\frac{\partial(RU)}{\partial X} + \frac{\partial(RV)}{\partial R} = 0 \tag{10}$$

$$\frac{\partial U}{\partial t} + U\frac{\partial U}{\partial X} + V\frac{\partial V}{\partial R} = Gr\,T + Gc\,C + \frac{1}{R}\frac{\partial}{\partial R}\left(R\frac{\partial U}{\partial R}\right) \tag{11}$$

$$\frac{\partial T}{\partial t} + U\frac{\partial T}{\partial X} + V\frac{\partial T}{\partial R} = \frac{1}{Pr}\left(1 + \frac{4}{3N}\right)\frac{1}{R}\frac{\partial}{\partial R}\left(R\frac{\partial T}{\partial R}\right) \tag{12}$$

$$\frac{\partial C}{\partial t} + U\frac{\partial C}{\partial x} + V\frac{\partial C}{\partial r} = \frac{1}{Sc}\frac{1}{R}\frac{\partial}{\partial R}\left(R\frac{\partial C}{\partial R}\right) \tag{13}$$

The corresponding initial and boundary conditions in non-dimensional quantities are given by

$$\begin{aligned} &t \leqslant 0 : U = 0,\ V = 0,\ T = 0,\ C = 0 \\ &\quad \text{for all } X \geqslant 0 \text{ and } R \geqslant 0 \\ &t \geqslant 0 : U = 1,\ V = 0,\ T = 1,\ C = 1 \\ &\quad \text{at } R = 1 \\ &U = 0,\ V = 0,\ T = 0,\ C = 0 \\ &\quad \text{at } X = 0 \text{ and } R \geqslant 1 \\ &U \to 0,\ T \to 0,\ C \to 0 \quad \text{as } R \to \infty. \end{aligned} \tag{14}$$

## 3. Numerical procedure

The governing Eqs. (10)–(13) are unsteady, coupled and non-linear with initial and boundary conditions (14). They are solved numerically by an implicit finite-difference method of Crank–Nicolson type which is stable and convergent as described in detail by Ganesan and Loganathan [8]. The region of integration is considered as a rectangle with sides $X_{max}(= 1.0)$ and $R_{max}(= 20)$ where $R_{max}$ corresponds to $R = \infty$ which lies very well outside the momentum, thermal and concentration boundary layers. The time-dependent equations are marched in time until a steady solution is obtained.

A convergence criterion based on the relative difference between the current and previous iterations is employed. When these differences are less than $10^{-5}$, the solution is assumed to have converged and iterative process is terminated. After experimenting with few set of mesh sizes, the mesh sizes have been fixed at the level $\Delta X = 0.02$, $\Delta R = 0.2$, with time step $\Delta t = 0.01$. In this case, spatial mesh sizes are reduced by 50% in one direction, and later in both directions, and results are compared. It is observed that, when the mesh size is reduced by 50% in the $R$-direction, the results differ in the fifth place after the decimal point while the mesh sizes are reduced by 50% in $X$-direction or in both directions the results are correct to fourth decimal places. Hence, the above mesh sizes have been considered as appropriate.

## 4. Results and discussion

The transient velocity, temperature and concentration profiles for different physical parameters such as $Gr$, $Gc$, $Sc$, $N$ and $Pr(= 0.71)$ are shown in Figs. 1–6 at $X = 1.0$. In Fig. 1, the steady-state velocity profiles are presented for different values of buoyancy force parameter $Gr$ or $Gc$ and $N$. For small values of $Gr = Gc(= 2)$, the time required to reach the steady-state with $N = 3$, 5 and 10 are 8.60, 9.44 and 9.65 respectively whereas for large $Gr = Gc(= 4)$ the steady-state is reached at 7.65, 8.48 and 8.69 respectively which leads to conclude that the increase in buoyancy force parameter $Gr$ or $Gc$, reduces the time to reach the steady-state. It can be seen that an increase in $N$ leads to a decrease in the velocity profiles are shown on Fig. 2 for different values of $Gr$ or $Gc$, $Sc$, $N$ and for fluid with Prandtl number $Pr(= 0.71)$. It reveals that the time required to reach the steady-state velocity is not affected by an increase in radiation parameter $N$. It is also concluded that the velocity decreases due to an increase in Schmidt number $Sc$. In these Figs. 1 and 2, $Sc(= 2.0)$ is larger than $Pr(= 0.71)$ and hence concentration layer is thinner than the thermal layer. This confines the downward flow to a thin region near the surface. For lower

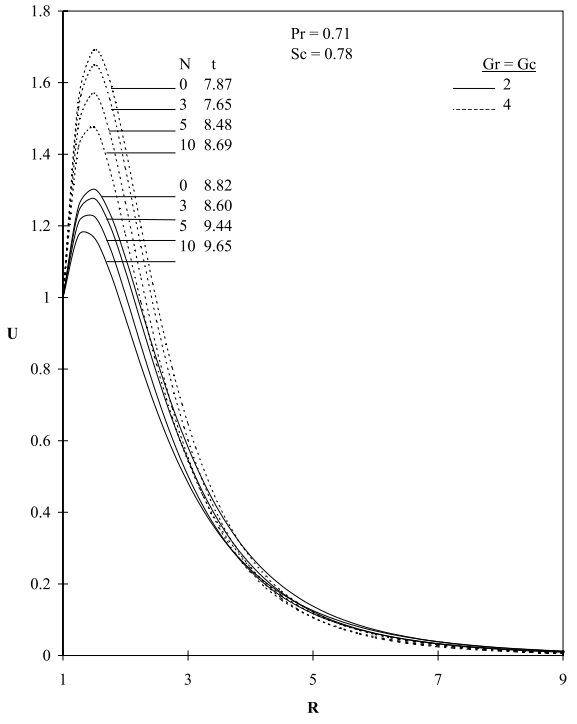


Fig. 1. Transient velocity profiles at $X = 1.0$ for different $Gr$, $Gc$ and $N$.

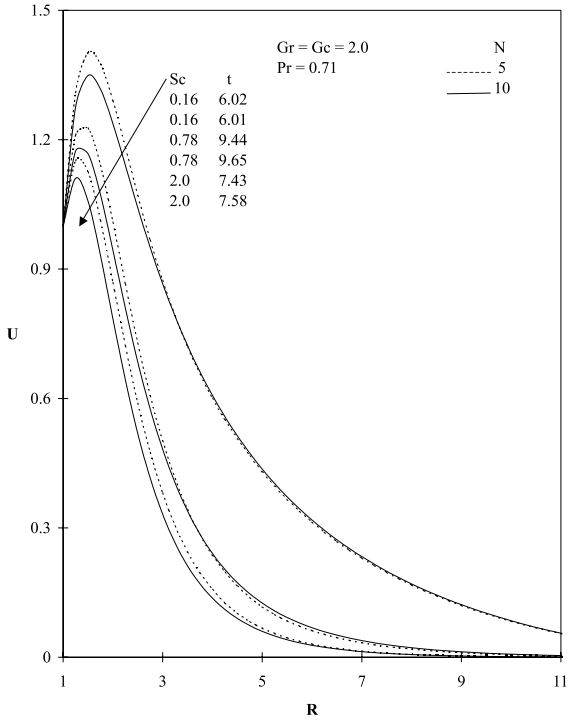


Fig. 2. Transient velocity profiles at $X = 1.0$ for different $Sc$.

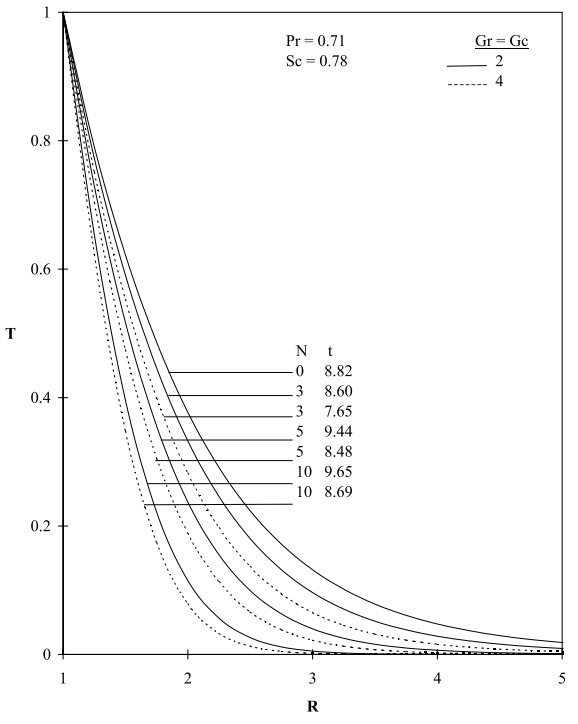


Fig. 3. Transient temperature profiles at $X = 1.0$ for different $Gr$, $Gc$ and $N$.

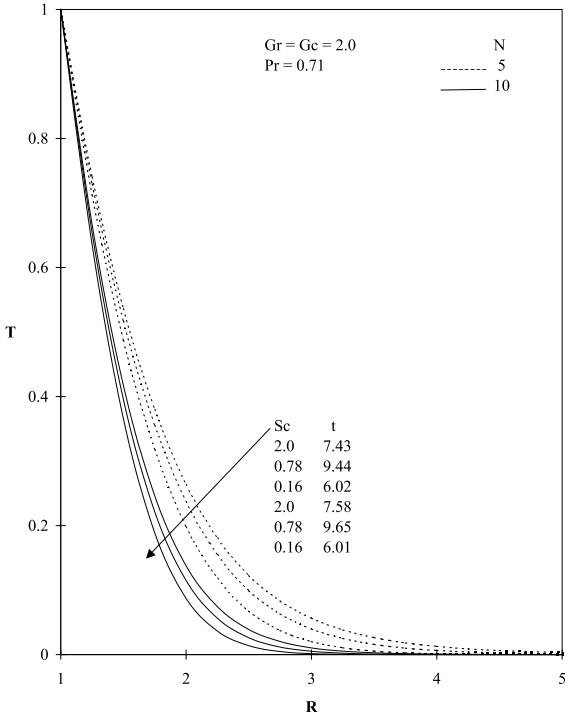


Fig. 4. Transient temperature profiles at $X = 1.0$ for different $Sc$.

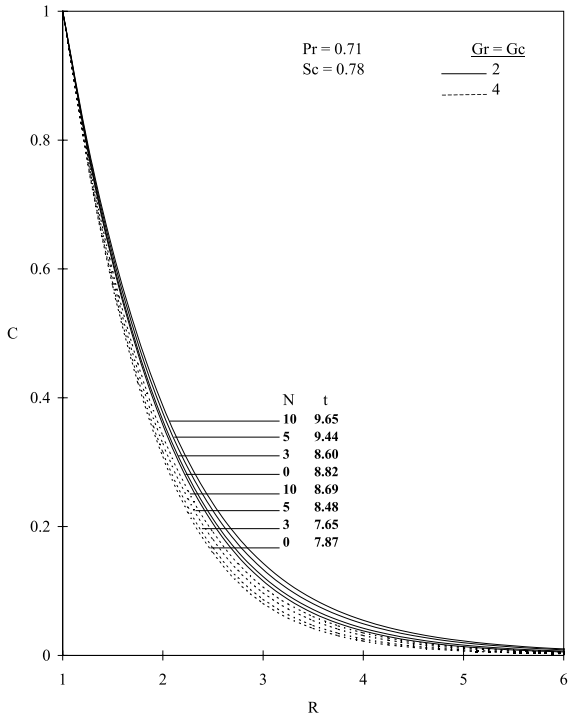


Fig. 5. Transient concentration profiles at $X = 1.0$ for different $Gr$, $Gc$ and $N$.

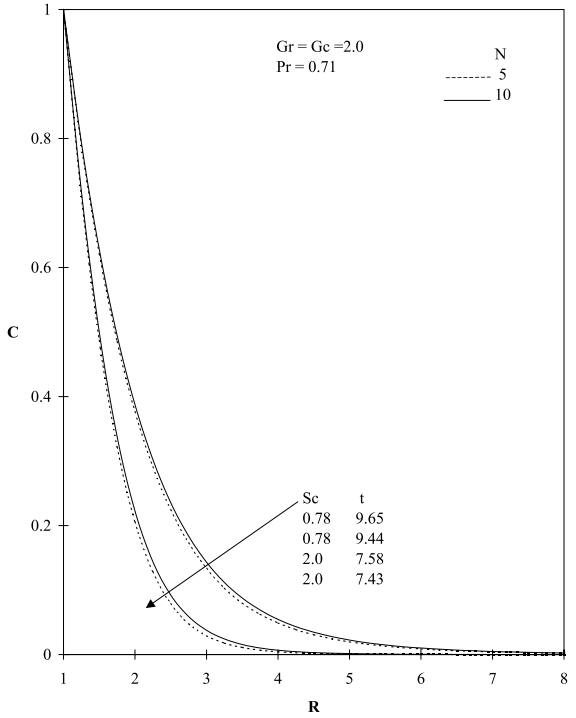


Fig. 6. Transient concentration profiles at $X = 1.0$ for different $Sc$.

$Sc$, the thickness of the concentration layer increases and the region of flow extend farther away from the cylinder.

Fig. 3 shows that the temperature increases with decreasing values of $Gr$ or $Gc$. In Fig. 4, it is seen that time required to reach steady-state temperature is more at higher values of $N(= 10)$ as compared to lower values of $N(= 5)$. It is observed that the temperature increases with increasing Schmidt number. From Figs. 1–4, it is observed that, owing to an increase in the value of the radiation parameter $N$, both the momentum and thermal boundary layer thickness decrease. However, the time taken to reach the steady-state increases as $N$ increases. At small values of $N$, the velocity and temperature of the fluid increases sharply near the cylinder as the time $t$ increase, which is totally absent in the absence of radiation effects.

The transient concentration profiles for $Pr = 0.71$, $Gr = Gc(= 2)$, $N = 5$, 10 and $Sc = 0.78$ and 2.0 are shown in Fig. 5. It is observed that for small values of $Sc = 0.78$ and $N = 5$, the time required to reach the steady-state is 9.44 whereas when $N = 10$, under similar conditions, the time required to reach the steady-state 9.65 from which it is conclude that for a higher value of $N$, the time taken to reach the steady-state is more when $Sc$ is small. It is also observed that increasing values of $N$ corresponds to a thicker concentration boundary layer relative to the momentum boundary layer. Hence, it can be noted that at high values of $Sc$, the time required to reach steady-state is less as compared to that at low values of $Sc$. Also, an increase in $Sc$ leads to a fall in the concentration. From Fig. 6, the effect of the buoyancy force parameter $Gr$ or $Gc$ on time to reach the steady-state conditions are shown graphically. For $Gr = Gc(= 2)$, the time required to reach the steady-state when $N = 3$, 5 and 10 are 8.60, 9.44 and 9.65 respectively whereas for large $Gr = Gc(= 4)$ the time required to reach the steady-state are 7.65, 8.48 and 8.69 respectively which leads to conclude that when the buoyancy force parameter $Gr$ or $Gc$ increases, the time required to reach the steady-state is reduced.

Knowing the velocity, temperature and concentration profiles, it is interesting to study the local and average skin-friction, the rate of heat transfer and mass transfer both in the transient and steady-state. The local as well as average skin-friction, Nusselt number and Sherwood number in terms of dimensionless quantities are given by

$$\tau_X = -(\partial U/\partial R)_{R=1} \tag{15}$$

$$\overline{\tau} = -\int_0^1 (\partial U/\partial R)_{R=1}\,\mathrm{d}X \tag{16}$$

$$Nu_X = -\frac{X(\partial T/\partial R)_{R=1}}{T_{R=1}} \tag{17}$$

$$\overline{Nu} = -\int_0^1 \left[\frac{(\partial T/\partial R)_{R=1}}{T_{R=1}}\right] \mathrm{d}X \tag{18}$$

$$Sh_X = -X(\partial C/\partial R)_{R=1} \tag{19}$$

$$\overline{Sh} = -\int_0^1 \left[(\partial C/\partial R)_{R=1}\right] \mathrm{d}X \tag{20}$$

The bar overhead denotes averages. The derivatives involved in Eqs. (15)–(20) are evaluated using five-point approximation formula and integrals are evaluated using Newton–Cotes formula.

Steady-state local skin-friction $\tau_X$ profiles are plotted in Fig. 7 against the axial coordinate $X$. The local shear stress $\tau_X$ increases with increasing value of $Sc$ and decreasing value of $Gr$ and $Gc$. The local Nusselt number $Nu_X$ for different $Gr$, $Gc$, $Sc$ and $N$ are shown in Fig. 8. Local heat transfer rate $Nu_X$ increases with decreasing values of $Sc$ and increases with increasing $Gr$ or $Gc$. For increasing value of radiation parameter $N$, the Nusselt number $Nu_X$ decreases. This trend is just opposite in case of local Sherwood number $Sh_X$ with respect to the $Gr$, $Gc$, $Sc$ and $N$ (Fig. 9).

Average values of skin-friction $\bar{\tau}$, Nusselt number $\overline{Nu}$ and Sherwood number $\overline{Sh}$ are shown in Figs. 10–12, respectively as a function of time at $X = 1.0$ for various values of physical parameters. In Fig. 10, it is noted that $\bar{\tau}$ decreases with decreasing value of $Sc$, but increases with decreasing value of $Gr$ or $Gc$ throughout the

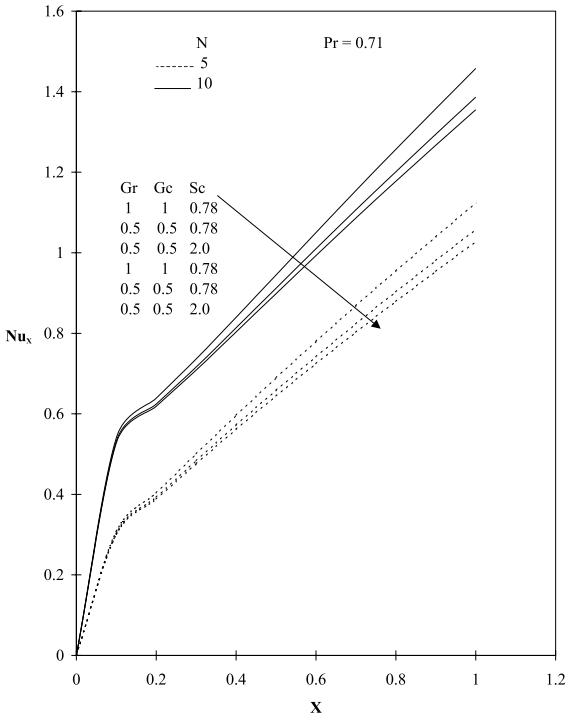


Fig. 8. Local Nusselt number.

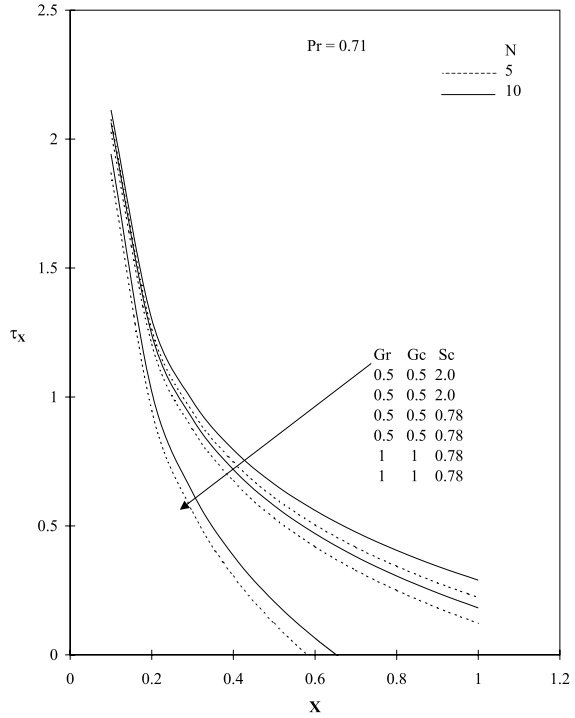


Fig. 7. Local skin-friction.

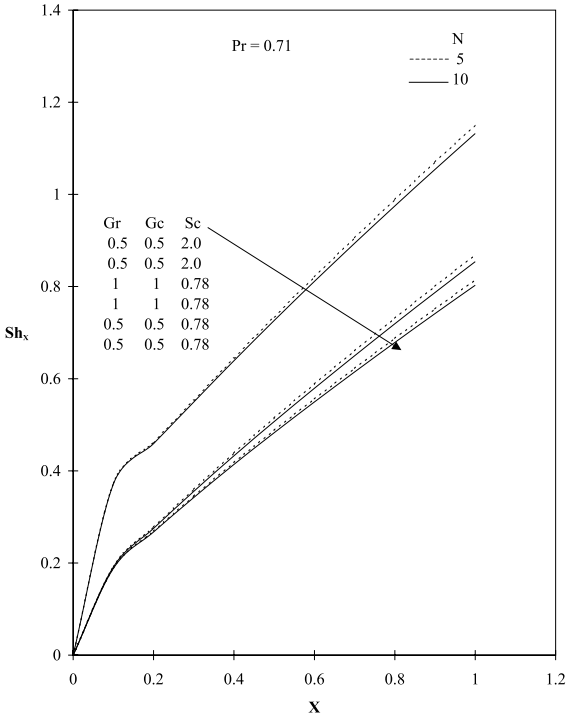


Fig. 9. Local Sherwood number.

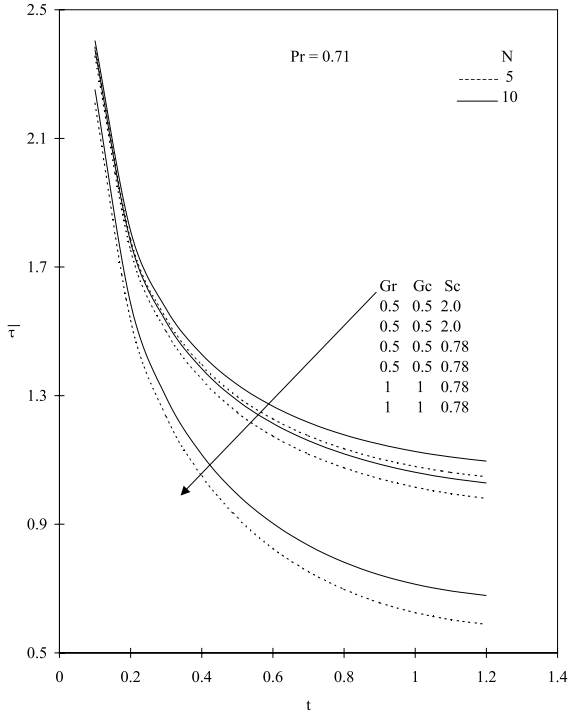


Fig. 10. Average skin-friction.

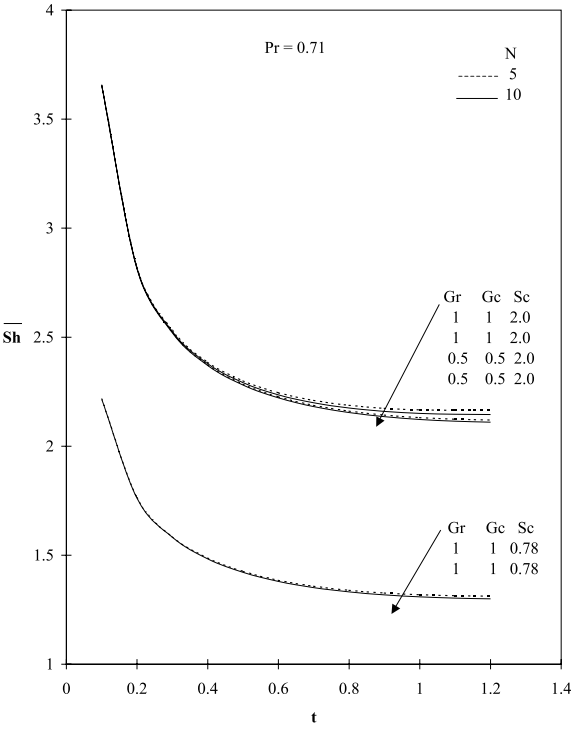


Fig. 12. Average Sherwood number.

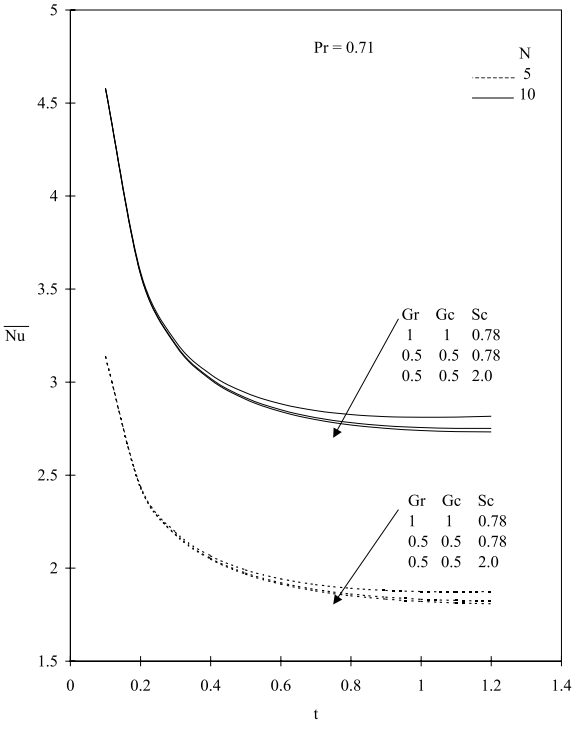


Fig. 11. Average Nusselt number.

transient period and at the steady-state level. It is also observed that the average skin-friction $\bar{\tau}$ increases as the radiation interaction parameter $N$ increases.

The average Nusselt number $\overline{Nu}$ increases with increasing values of $Gr$ or $Gc$ and $N$. There is no change in average Nusselt number in the initial period with respect to $N$. This shows that initially there is only heat conduction. In Fig. 12, the Sherwood number $\overline{Sh}$ increases as $Gr$ or $Gc$ and $Sc$ increases. The effect of $Sc$ is more on average Sherwood number $\overline{Sh}$. In the initial period it is observed that there is no change in average Sherwood number $\overline{Sh}$ with respect to $Gr$ or $Gc$ and $Sc$.

## 5. Conclusion

A numerical study has been carried out to study the radiation effects on flow past an impulsively started semi-infinite vertical cylinder in the presence of mass transfer. The fluid is a gray, absorbing–emitting but non-scattering medium and the Rosseland approximation is used to describe the radiative heat flux in the energy equation. A family of governing partial differential equations is solved by an implicit finite-difference scheme of Crank–Nicolson type, which are stable and convergent. The results are obtained for different values of radiation parameter $N$, Prandtl number $Pr$, thermal

Grashof number $Gr$, modified Grashof number $Gc$ and Schmidt number $Sc$. Conclusions of this study are as follows:

1. The time required to reach the steady-state increases as radiation parameter $N$ increases.
2. The momentum boundary layer thickness increases with decreasing values of $Sc$. It is observed that there is a rise in the velocity due to the presence of mass diffusion.
3. At small values of the radiation parameter $N$, the velocity and temperature of the fluid increases sharply near the cylinder as the time $t$ increase, which is totally absent in the absence of radiation effects.
4. A higher value of $N$ corresponds to a thinner concentration boundary layer relative to the momentum boundary layer. This results in a larger concentration gradient on the cylinder.
5. The local and average skin-friction $\bar{\tau}$ increases with decreasing $Gr$ or $Gc$ and increases with increasing value of $N$ and $Sc$.
6. The average Nusselt number $\overline{Nu}$ increases with increasing value of radiation parameter $N$ and decreasing values of $Sc$.
7. The Sherwood number $\overline{Sh}$ increases as $Gr$ or $Gc$ and $Sc$ increases.

## Acknowledgements

The second author wishes to acknowledge the support for this research work from CSIR (Council of Scientific and Industrial Research) through the award of Senior Research Fellowship.

## References

[1] V.S. Arpaci, Effects of thermal radiation on the laminar free convection from a heated vertical plate, Int. J. Heat Mass Transfer 11 (1968) 871–881.
[2] J.D. Bankston, J.R. Lioyed, J.L. Novony, Radiation convection interaction in an absorbing–emitting liquid in natural convection boundary flow, J. Heat Transfer ASME C99 (1977) 125–127.
[3] M.Q. Brewster, Thermal Radiative Transfer and Properties, John Wiley & Sons. Inc., New York, 1992.
[4] R.D. Cess, Interaction of thermal radiation with free convection heat transfer, Int. J. Heat Mass Transfer 9 (1966) 1269–1277.
[5] E.H Cheng, M.N. Ozisik, Radiation with free convection in an absorbing emitting and scattering medium, Int. J. Heat Mass Transfer 15 (1972) 1243–1252.
[6] A.C. Cogley, W.C. Vincenti, S.E. Gilles, Differential approximation for radiative transfer in a non-gray gas near equilibrium, Am. Inst. Aeronaut. Astronaut. J. 6 (1968) 551–555.
[7] U.N. Das, R. Deka, V.M. Soundalgekar, Radiation effects on flow past an impulsively started vertical plate-an exact solutions, J. Theo. Appl. Fluid Mech. 1 (2) (1996) 111–115.
[8] P. Ganesan, P. Loganathan, Unsteady free convection flow over a moving vertical cylinder with heat and mass transfer, Heat Mass Transfer 37 (1) (2001) 59–65.
[9] R. Grief, I.S. Habib, J.C. Lin, Laminar convection of a radiating gas in a vertical channel, J. Fluid Mech 46 (1971) 513–520.
[10] M.A. Hossain, H.S. Takhar, Radiation effects on mixed convection along a vertical plate with uniform surface temperature, Heat Mass Transfer 31 (1996) 243–248.
[11] M.A. Hossain, H.S. Takhar, Thermal radiation effects on the natural convection flow over an isothermal horizontal plate, Heat Mass Transfer 35 (1999) 321–326.
[12] M.A. Hossain, M. Kuttubuddin, I. Pop, Radiation–conduction interaction on mixed convection from a horizontal circular cylinder, Heat Mass Transfer 35 (1999) 307–314.
[13] M.A. Monsour, Radiation and free-convection effects on the oscillating flow past a vertical plate, Astrophys. Space Sci. 166 (1990) 269–275.
[14] J.L. Novotny, M.D. Kelleher, Free-convection stagnation flow of an absorbing–emitting gas, Int. J. Heat Mass Transfer 10 (1967) 1171–1178.
[15] A. Raptis, C. Perdikis, Radiation and free convection flow past a moving plate, Appl. Mech. Eng. 4 (4) (1999) 817–821.
[16] A. Raptis, Radiation and free convection flow through a porous medium, Int. Comm. Heat Mass Transfer 25 (2) (1998) 289–295.
[17] H.S. Takhar, A.J. Chamkha, G. Nath, Combined heat and mass transfer along a vertical moving cylinder with a free stream, Heat Mass transfer 36 (2000) 237–246.
[18] K.A. Yih, Radiation effect on natural convection over a vertical cylinder embedded in porous media, Int. Comm. Heat Mass Transfer 26 (2) (1999) 259–267.